Recalculation of Astrophysical Opacities: Overview, Methodology and Atomic Calculations

Anil K. Pradhan & Sultana N. Nahar

The Ohio State University, Columbus, Ohio, USA 43210

pradhan.1@osu.edu

Abstract.

A review of a renewed effort to recalculate astrophysical opacities using the R-Matrix method is presented. The computational methods and new extensions are described. Resulting enhancements found in test calculations under stellar interior conditions compared to the Opacity Project could potentially lead to the resolution of the solar abundances problem, as well as discrepancies between recent experimental measurements at the Sandia Z-pinch inertial confinement fusion device and theoretical opacity models. Outstanding issues also discussed are: (i) accuracy, convergence, and completeness of atomic calculations, (ii) improvements in the Equation-of-State of high-temperature-density plasmas, and (iii) redistribution of resonant oscillator strength in the bound-free continuum, and (iv) plasma broadening of auotionizing resonances.

1. Introduction

The Opacity Project was launched in 1983 with the goal of calculating astrophysical opacities using state-of-the-art atomic physics based on the coupled channel (CC) approximation employing the powerful R-Matrix (RM) method (Seaton *et al.* 1994, *The Opacity Project Team* 1995, 1996). Over the next decade, a suite of extended RM opacity codes were developed to compute large-scale bound-bound transition strengths and bound-free photoionization cross sections with unprecedented accuracy One of the primary features of OP was the precise delineation of intrinsic autoionizing resonance profiles whose shapes, extent and magnitudes are determined by myriad channel couplings in the (electron+ion) system. However, CC-RM calculations are of immense complexity and require substantial computational effort and resources. For the often dominant inner-shell transitions they could not be completed owing to computational constraints on the then available high-performance supercomputing platforms. Simpler approximations akin to distorted-wave (DW) type methods used in other opacity models that neglect channel couplings, were therefore employed to compute most of the OP data.

In recent years a renewed effort has been under way as originally envisaged using the CC-RM methodology (Nahar and Pradhan 2016a; hereafter NP16a), stimulated by two independent developments. The first was a 3D Non-LTE analysis of solar elemental abundances that were up to 50% lower for common volatile elements such as C, N , O and Ne (Asplund *et al.* 2009). It was suggested that an enhancement of up to 30% in opacities could resolve the discrepancy, particularly in helioseismological models (Bahcall *et al.* 2005; Basu and Antia 2008; Christensen-Dalsgaard *et al.* 2009; J. Bah-

call, private communication). The second was an experimental measurement of iron opacity at the Sandia Z-pinch inertial confinement fusion device, under stellar interior conditions prevalent at the base of the solar convection zone (BCZ), that were 30-400% higher in monochromatic opacity compared to OP (Bailey *et al.* 2015). The Z-pinch results for the Rosseland Mean Opacity (RMO) were also substantially higher using the measured data, and found nearly half the enhanecment needed to resolve the solar abundance problem.

The pilot CC-RM calculations in NP16 for an important iron ion Fe XVII resulted in 35% enhancement relative to the OP RMO at the Z conditions. While the enhancement is consistent with subsequently reported results from other opacity models (Blancard *et al.* 2016, Nahar and Pradhan 2016b), there are also important differences in (i) atomic physics, (ii) equation-of-state, and (iii) plasma broadening of autoionizing resonances. The Fe XVII calculations were carried through to convergence by including n = 3 and n = 4 levels of the target ion FeXVIII. They showed large enhancements in photoionization cross sections, as successive thresholds are included, due to coupled resonance structures and the background. The extensive role of photoionization-of-core (PEC) or Seaton resonances (Yu and Seaton 1987) associated with strong dipole transitions in the core ion Fe XVIII is especially prominent (NP16a). Several other sets of the pilot calculations have been carried out: relativistic Breit-Pauli R-Matrix (BPRM) calculations incluging 60 fine structure levels up to the n = 3 thresholds, non-relativistic calculations including 99 LS terms up to the n = 4 threshold, as well as BPRM calculations with 218 fine structure levels (in progress). One of the aims is to benchmark existing DW cross sections and monochromatic opacities in the non-resonant background and the high energy region above all coupled excitaion thresholds.

Among the compromises necessary at the time of the intial OP work related to very small wavefunction expansions for the (e + ion) system in R-Matrix calculations, usually limited to the ground configuration of the core ion. One of the main points of the NP16a work was that *in general for any atomic system a converged expansion in terms of the target configurations and levels is needed to include the full enhancement of photionization cross sections for each level in the bound free continuum*.

We are also investigating occupation probabilities from the Mihalas-Hummer-Dappen equation-of-state employed in the OP work which are orders of magnitude lower for excited levels than other models.

A new theoretical method and computational algorithm for electron impact broadening of autoionizing resonances in plasmas, as function of temperature and density, is described [9]. Finally, issues related to completeness and accuracy are addressed [6,10].

Following sections describe some of the salient features of the work outlined above.

2. Close coupling and distorted wave approximations

The Close-Coupling approximation is implemented using the R-Matrix method (CC-RM). It involves the expansion of the total wavefunction for the (electron + ion) system in terms of the eigenfunctions of the “target" or the “core" ion states and a free electron wavefunction.

$$\Psi(E) = A \sum_i \chi_i \theta_i + \sum_j c_j \Phi_j, \tag{1}$$

where χ_i is the target ion wave function in a specific state $S_i\ L_i$ and θ_i is the wave function for the free electron in a channel labeled as $S_i L_i k_i^2 \ell_i (S L\pi)$; k_i^2 being its incident kinetic energy. In contrast to the CC-RM method, the DW approximation, used in existing opacity models, neglects the summation over hundreds to thousands of channels on the RHS. In essence that implies that the DW method neglects the quantum superposition and interference that gives rise to autoionizing resonances in an *ab initio* manner. To obtain bound-bound, bound-free, and scattering matrix elements, we obtain (e+ion) wavefunctions $\Psi_B(S L\pi; E)$ and $\Psi_F(S L\pi; E')$. For bound states B and B' the line strength in a.u. is given by $\Gamma(B; B') = | < \Psi_B(E_B)\|\mathbf{D}\|\Psi_{B'}(E_{B'}) > |^2$, where **D** is the dipole operator. If the final state is a continuum state represented by $\Psi_F(E')$ and the initial state by $\Psi_B(E)$ then the photoionization cross section is given by $\sigma_\omega(B; E') = \frac{4}{3}\frac{\alpha\omega}{g_i}| < \Psi_B(E_B)\|\mathbf{D}\|\Psi_F(E') > |^2$ where ω is the photon frequency and E' is the energy of the outgoing electron. The relativistic BPRM method incorporates the Breit-Pauli Hamiltomian for the (N+1)-electron system. We employ a pair-coupling representation $S_i L_l(J_i) l_i(K_i) s_i(J\pi)$. As the individual states $S_i L_i$ split into the fine structure levels J_i, the number of channels becomes several times larger than the corresponding LS coupling case. Hitherto, the version of BPRM codes included only the 1-body terms of the Breit interaction, namely the spin-orbit (so) coupling, mass correction (m), and Darwin (d) terms (Eissner 1991). Chen and Eissner (to be published) have developed an improved Breit-Pauli version including the 2-body terms in the Breit interaction (Fig. 1), that should be more accurate for fine structure and resonance effects in the Fe-group elements.

3. R-Matrix Opacity Codes

The R-Matrix opacity codes (Seaton 1987, Berrington *et al.* 1987) are significantly different from the original R-Matrix codes (Burke 2011), and have been considerably extended by the OSU group for complete RM opacity calculations (Fig. 1, Fig. 2). Fig. 1 is a flow-chart of the RM codes set up and used by the PI and collaborators at the Ohio Supercomputer Center (OSC) since 1990. An accurate configuration interaction representation or the core ion states is obtained by two atomic structure codes, **SUPERSTRUCTURE** (Eissner *et al.* 1974) and **CIV3** (Hibbert 1975). The first two R-matrix codes, **STG1,STG2**, are then employed to generate the multipole integrals, algebraic coefficients and set up the (N+1)-electron Hamiltonian corresponding to the coupled integro-differential equations. The Hamiltonian is diagonalized in **STGH**; in the BP calculations the diagonalization is preceded by LSJ recoupling in **RECUPD**. The R-matrix basis set of functions and the dipole matrix elements so produced are then input into **STGB** for bound state wavefunctions, **STGF** for continuum wavefunctions, **STGBB** for radiative transition probabilities, and **STGBF** for photoionization cross sections. In addition, **STGF(J)** is used to obtain collision strengths for electron impact excitation in LS or intermediate coupling and fine structure transitions.

The flowchart of the new package of codes for opacities calculations is shown schematically in Fig. 1; each of the boxes represents a series of subsidiary codes. The new version of the R-Matrix opacities codes is the extension of following codes under

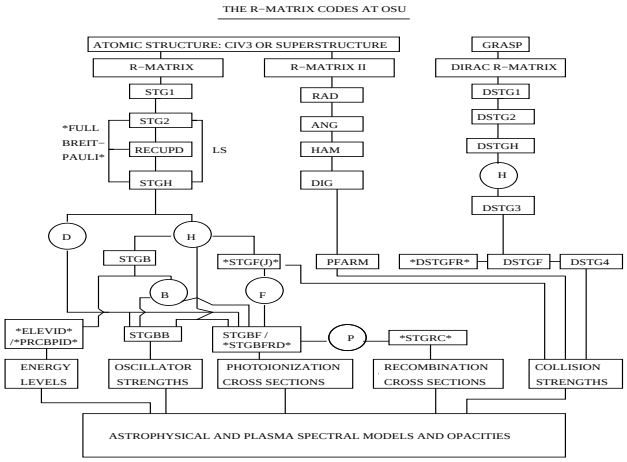

Figure 1. The R-Matrix codes for calculation of opacities. The left branch of Breit-Pauli codes is employed in the results presented in this work.

development: (A) INTFACE — to interface atomic data for bound-free photoionization and bound-bound transition probabilities including relativistic fine structure, and (B) AUTOBRO — an algorithm for electron impact broadening of autoionizing resonances with a temperature-density dependent kernel, HIPOP — high-precision version of the opacities code with high-resolution (10^5 frequencies) and monochromatic opacities and Rosseland and Planck means for arbitrary mixtures. The database OPSERVER is described by Mendoza *et al.* (2007); its updated version has been established at CDS by F. Delahaye.

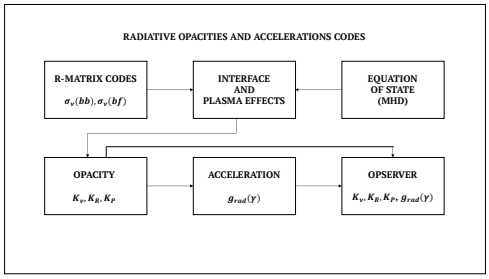

Figure 2. The opacity codes including interfacing with CC-RM data and the equation-of-state calculations.

4. Inner- and outer-shell excitations

The CC-RM approach entails an increasing succession of open channels as each threshold of the core ion is approached from below (Eq. 1). As the number of free channels (open + closed) multiplies, the sizes of the (e + ion) algebra and R-Matrix diagonalization matrices and arrays may become very large. In addition, there are issues related to spectroscopic identification of a highly excited and mixed-configuration bound (e + ion) levels from STGB calculations, and subsequent bound-bound STGBB and bound-free STGBF calculations (Fig.1). While these have been solved, they require commensurate computational resources and expertise.

Inner-shell excitations using the DW method have been described in earlier works (e.g. Badnell and Seaton 2003). Despite that fact that most of current OP data was computed using variants of DW data, the initial OP calculations were done using the RM method, albeit with relatively small eigenfunction expansion and only few outer-shell excitations. Most of OP codes were originally developed to employ the RM methodology, but computational constraints precluded OP work from incorporating resonant inner-shell atomic processes that manifest themselves strongly in the *bound-free* cross sections. But inner-shell excitations are dominant contributors to opacity because most electrons in complex ions are in closed shells, whose excitation energies lie above the (first) ionization threshold. Much of the opacity therefore lies in the strongest such transitions that are associated with dipole transitions in the core of the ion. The corresponding autoionizing resonances are referred to as *Photoexciation-of-Core* (PEC) or Seaton resonances (Yu and Seaton 1987, Nahar *et al.* 2011, NP16; and discussed extensively in *Atomic Astrophysics and Spectroscopy*, Pradhan and Nahar 2011). *The PEC resonances are the largest single contributing feature to the bound-free opacity.* Therefore, their simple treatment as bound-bound transitions in current DW opacity models needs verification.

5. New R-Matrix opacity calculations: Test case of Fe XVII

The monochromatic opacity comprises of bound-bound (bb), bound-free (bf), free-free (ff) and photon scattering (sc) contributions:

$$\kappa_{ijk}(\nu) = \sum_k A_k \sum_j f_j \sum_{i,i'} [\kappa_{bb(}(i,i';\nu) + \kappa_{bf}(i,\epsilon i';\nu) + \kappa_{ff}(\epsilon i,\epsilon' i';\nu) + \kappa_{sc}(\nu)], \quad (2)$$

where A_k is the abundance of element k, f_j the ionization fraction j, i, i' are the initial bound and final bound or continuum states of the atomic species, and ϵ represents the electron energy in the continuum. The Rosseland Mean Opacity (RMO) κ_R is defined in terms of $\kappa_{ijk}(\nu)$ as

$$\frac{1}{\kappa_R} = \frac{\int_0^\infty g(u)\frac{1}{\kappa_\nu}du}{\int_0^\infty g(u)du}, \quad g(u) = u^4 e^{-u}(1-e^{-u})^{-2}, \quad (3)$$

where $g(u)$ is the derivative of the Planck weighting function (corrected for stimulated emission), $\kappa_\nu^{bb}(i \rightarrow j) = \left(\frac{\pi e^2}{m_e c}\right) N_i f_{ij} \phi_\nu$, and $\kappa_\nu^{bf} = N_i \sigma_\nu$. The κ_ν is primarily a function of the *bb* oscillator strengths f, *bf* photoionization cross sections σ_ν, level populations N_i, and the line profile factor ϕ_ν.

The CC-RM computational framework for large-scale computations comprises mainly the first two components of the opacity on the RHS of Eq. 2 (i) the bound-bound (bb) transition probabilities, and (ii) photoionization of bound-free (bf) cross sections.

We focus on test calculations for an important contributor to opacity at the Z-pinch plasma conditions: $T = 2.11 \times 10^6$K and $N_e = 3.1 \times 10^{22}$ cc; the experimental energy range and the range of the Planck function derivative dB/dT is shown in Fig. 3 (Right). The Fe XVII calculations involved coupled channel wavefunction expansion in Eq. 1 including 30 LS terms with 60 fine structure levels up to the $n \leq 3$ complex of the core ion Fe XVIII (Nahar *et al.* 2011), and 99 LS terms or 218 levels up to $n \leq 4$ (NP16a); the latter calculation was an order of magnitude larger computationally. The associated $n = 2 \rightarrow 3$ core transitions in Fe XVIII in the former case, and $n = 2 \rightarrow 3, 4$ in the latter case, give rise to numerous PEC resonances in the bound-free photoionization cross sections of Fe XVII. Fig. 3 (Left) from NP16a compares enhancement in the new cross sections compared to 2-state coupled channel results from OP that reproduce only the background. There is no "misrepresentation" of OP as asserted by Iglesias and Hansen (2017; hereafter IH17), since that is the only other CC calculation available; rest of the OP work is DW.

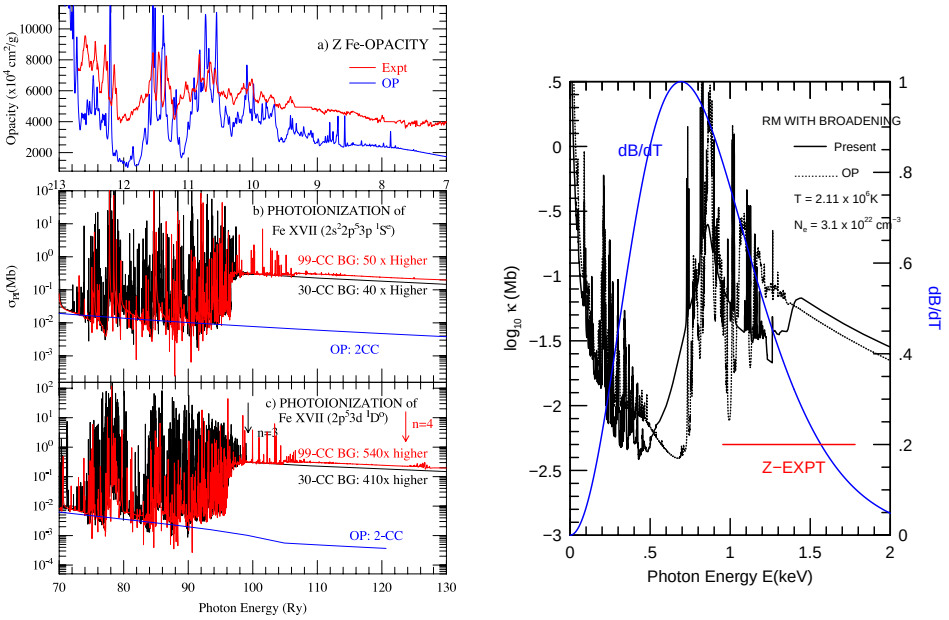

Figure 3. *Left*: Autoionizing resonance structures in R-Matrix photoionization cross sections of two Fe XVII excited levels (bottom and middle panels); "higher-than-predicted" Sandia Z-pinch measurements of total Fe opacity (top panel, Bailey *et al.* 2015). Calculations are needed for Fe XVI-XXI to compare with experiments at Z plasma conditions. *Right:* Monochromatic R-Matrix opacity of Fe XVII at T = 2.11×10^6K and $N_e = 3.1 \times 10^{22}$ cm^{-3}, corresponding to total iron opacity measurements at the Sandia Z-pinch fusion device in the energy range shown by the red bar (Fig. 3, Left); the R-Matrix Fe XVII RMO is ~60% higher than the OP (Table 1).

6. Convergence and completeness

The two criteria for *accuracy and completeness* of RM opacity calculations are: (I) **convergence** of wavefunction expansion (Eq. 3) with respect to bound-free cross sections and bound-bound transition probabilities, and (II) **completeness** of monochromatic and RMOs with respect to a very large number of possible multiply excited configurations that contribute to the background non-resonant cross sections in high-temperature plasmas. The NP16a work demonstrated convergence with respect to the Fe XVIII target ion included in the CC-RM calculations (Fig. 3, Left), but the highly excited configurations were not included that affect the high-energy behavior.

Although the number of these excited configurations is large, their contribution to opacity is still small relative to the main CC-RM cross sections. It is also specific to the energy range where the quasi-degenerate configurations lie. In addition, they represent the background contribution without resoances; thus amenable to simpler approximations such as the DW without loss of accuracy. We refer to these configurations as "top-up" contribution to the CC-RM calculations.

Whereas enumerating excited configurations is straightforward in atomic structure-DW calculation (IH17 and Zhao *et al.* in this volume), it is more complex and indirect in CC-RM calculations owing to resonant phenomena (IH17 incorrectly state that some of the configurations were omitted in NP16a; in fact the $nl = 4d, 4f$ are included). For example, the 60CC n$\leq$ 3 BPRM calculations yield 454 bound levels of Fe XVII, but we have further included $> 50,000$ topup levels to compute the opacity spectrum in Fig. 3 (Right). However, the photoionization cross sections of the 454 strictly bound levels (-ve energy eigenvalues) includes embedded autoionizing resonances that are treated as distinct levels in the DW calculations. Therefore, in total there are commensurate number of levels to ensure completeness. Zhao *et al.* discuss the complementary topup to the CC-RM calculations and find a $\sim$20% increment. Satisfying both these criteria results in a further enhancement in the Fe XVII RMO over those obtained in NP16a of $\sim$ 60% over OP. Table 1 shows the latest CC-RM results compared to other models. We expect additional enhancement upon completion of the n=4 fine structure calculations, that is likely the cause of the deficit in monochromatic opacity just below 1.5 keV in Fig. 3 (Left); updated results will be presented in Pradhan *et al.* (2017).

Table 1. Comparison of recent R-Matrix results (Pradhan *et al.* 2017) with other opacity models for Fe XVII employing variants of the DW method (Blancard *et al.* 2016), are over 60% higher; further enhancement in R-Matrix opacities is expected after proposed improvements in more extended atomic calculations and the MHD-EOS.

Opacity Enhancement Factors for Fe XVII relative to OP	
R-Matrix (Pradhan *et al.* 2017)	1.64
OPAS (Blancard *et al.* 2012)	1.55
SCO-RCG (Blenski *et al.* 2000)	1.37
ATOMIC (Magee *et al.* 2013)	1.32
SCRAM (Hansen *et al.* 2007)	1.27
TOPAZ (Iglesias 2015)	1.21

7. Differential oscillator strength distribution and sum-rule

The oscilltor strength sum-rule is invoked to ensure completeness. The summation over all bound-bound and bound-free transitions must satisfy the condition built into the definition of the oscillator strength as a fractional probability of excitation; Ergo: $\sum_j f_{ij} = N$, where N is the number of active electrons. However, while the f-sum rule ensures completeness, it does not relate to the accuracy of atomic calculations per se. Rather, it is the precise energy distribution of differential oscillator strength that is the determinant of accuracy. To wit: a hydrogenic approximation for complex atoms would satisfy the f-sum rule, but it would clearly be inaccurate. As demonstrated above, the CC-RM method is concerned primarily with differential oscillator strength in the bound-free continuum that, in turn, depends on delineation of auotionizing resonances.

Similarly, the RMO depends on the energy distribution monochromatic opacity via the Planck function at a given temperature. Fig.3 (Right) shows dB/dT at the Z-pinch temperarture of 2.11 $\times 10^6$K. Compared with the OP results, the distribution of the CC-RM Fe XVII monochromatic opacity is quite different and much more smoothed out, without the sharp variations that stem maily from the treatment of resonances as bound-bound lines (albeit inclusion of limited autoionization broadening perturbatively in the DW approximation. The flatter distribution is also observed experimentally, in contrast to theoretical opacity models that exhibit "opacity windows" (Fig.3, Left).

8. Plasma broadening of autoionizing resonances

An unsolved atomic physics problem is the broadening of autoionizing resonances by plasma effects, line broadening theory which is well developed and extensively considered in existing opacity calculations. But since autoionizing resonance shapes are not considered, neither is their broadening as function of density and temperature. However, the distribution of differential oscillator strength and the structure of the bound-free opacity depends critically on how resonances broaden and dissolve into the continuum from the CC-RM calculations.

At high densities the dominant form of plasma broadening is due to electron impact. We have developed an algorithm implemented in the INTFACE code (Fig. 2), prior to opacity calculations (Pradhan 2017). Fig. 4 shows electron impact broadening of autoinizing resonances in a typical CC-RM photoionization cross section at two temperatures, 10^6 and 10^7K, and a range of densities: $N_e = 10^{20}$ cc where the onset of broadening is discernible, to high densities $N_e = 10^{23}$ cc where the resonance structures are mostly dissolved into the continuum. The broadening profiles are normalized Lorentzian, with no effect on the non-resonant continuum, viz. Fig. 3 (Right).

9. Equation-of-State

The Mihalas-Hummer-Däppen equation-of-state (MHD-EOS) was formulated for OP (Mihalas *et al.* 1988; *The Opacity Project Team* 1995). The MHD "chemical picture" treats isolated atoms, for which the CC-RM data are computed, perturbed by plasma environment via occupation probabilities w_i in the atomic internal partition function

$$U(i, j, k) = \sum_i w_i g_i exp(-E_i/kT), \tag{4}$$

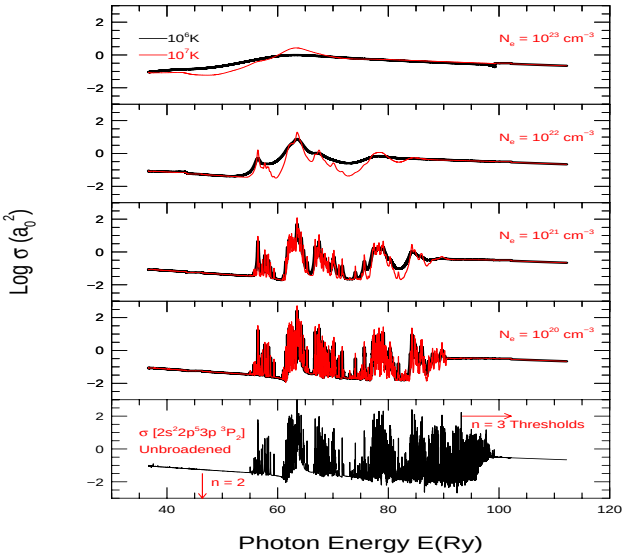

Figure 4. Plasma broadening of autoionizing resonances with temperature and densities, bottom panel — unbroadened cross section, upper panels — dissolution of resonance structures into the bound-free continuum with increasing density at T = 10^6K (black) and 10^7K (red).

.

and the modified Boltzmann-Saha equation; E_i is the excitation energy of level i, g_i its statistical weight, and T the temperature. The w_i are determined upon free-energy minimization of the plasma at a given temperature-density. An atomic level i is considerd dissolved by the plasma microfields when its highest Stark sub-level overlaps with the lowest sub-level of the $i + 1$ level. The MHD-EOS originally stipulated a stringent validity criterion for mass densities $\rho \leq 0.01$ g/cc valid for stellar envelopes (Seaton *et al.* 1994). But that is insufficient even to reach the solar BCZ depths *rho* ≥ 0.1 g/cc. Nevertheless, a modified version named Q-MHD it has been employed in the OP work, with W_i cut-offs at very high densities An unresolved problem has also been that the chemical picture level populations are orders of magnitude lower (Badnell and Seaton 2003) than the physical picture EOS utilized in the Livermore opacity calculations (Rogers and Iglesias 1992). An improved treatment of these issues in the high-density regime has been developed by Trampedach *et al.* (2006), and would be incorporated in the new RM opacity calculations.

Another issue pertains to topup levels referred to above, in addition to the CC-RM levels. Including a large number of levels in the MHD-EOS drastically affects the overall population distribution since it is normalized via the internal partition function (Eq. 4). To wit: the ground state of Fe XVII ends up with no more than a few percent of the population at Z-pinch plasma and BCZ conditions. It is expected that the improved method by Trampedach *et al.* would also alleviate this problem.

10. Conclusion

The R-Matrix opacity calculations described in this review are difficult and time consuming, but ensure high accuracy using state-of-the-art atomic physics, as originally envisioned in the OP. Furthermore, the CC-RM calculations are needed to verify existing opacity models that employ some variant of the simpler DW method, but with large differences of ~30% or more among them (viz. Table 1). Ongoing and planned laboratory experiments at the Sandia Z-pinch and the Livermore National Ignition Facility (T. Perry in this volume) should also serve to validate theoretical models to resolve outstanding discrepancies and fundamental issues in atomic physics, astrophysics and plasma physics.

Acknowledgments. We would like to thank Werner Eissner, Regner Trampedach, Lianshui Zhao and Chris Orban for contributions. This work was partially supported by the U.S. Department of Energy and the U.S. National Science Foudnation. The computational work was carried out primarily at the Ohio Supercomputer Center in Columbus, Ohio.

References

M. Asplund, N. Grevesse, A. J. Sauval and P. Scott, *Ann. Rev. Astro. Astrophys.* 47, 481 (2009).
N.R. Badnell and M.J. Seaton, *J. Phys. B* , 36, 4367 (2003).
J.N. Bahcall, S. Basu, M.H. Pinsonneault, A.M. Serenelli, *Astrophys. J.* , 618, 1049 (2005).
J. E. Bailey, T. Nagayama, G. P. Loisel, G. A. Rochau, C. Blancard, J. Colgan, Ph. Cosse, G. Faussurier, C. J. Fontes, F. Gilleron, I. Golovkin, S. B. Hansen, C. A. Iglesias, D. P. Kilcrease, J. J. McFarlane, R. C. Mancini, S. N. Nahar, C. Orban, J.-C. Pain, A. K. Pradhan, M. Sherill & B. G. Wilson, Nature, 517, 56-59 (2015).
S. Basu and H.N. Antia, Physics Reports, 457, 217 (2008).
C. Blancard, J. Colgan, Ph. Cosse, G. Faussurier, C.J. Fontes, F. Gilleron, I. Golovkin, S.B. Hansen, C.A. Iglesias, D.P. Kilcrease, J.J. MacFarlane, R.M. More, J.-C.Pain, M. Sherrill and B.G. Wilson, *Phys. Rev. Lett.* 117, 249501 (2016).
P.G. Burke, *R-Matrix Theory of Atomic Collisions*, Springer Series on Atomic, Optical and Plasma Physics (2011).
J. Christensen-Dalsgaard, M. P. Di Mauro, G. Houdek, and F. Pijpers, *Astron. Astrophys.* , 494, 205 (2009).
W. Eissner, M.Jones, H. Nussbaumer *Comput. Phys. Commun.* 8, 270 (1974).
C.A. Iglesias and S.B. Hansen, apj 835, 284 (2017).
C. Mendoza, M.J. Seaton, P. Buerger, A. Bellorin, M. Melendez, J. Gonzalez, L.S. Rodriguez, E. Palacios, A.K. Pradhan, C.J. Zeippen, *Mon. Not. R. astr. Soc.* , 378, 1031 (2007).
D. Mihalas, W. Däppen, and D.G. Hummer, *Astrophys. J.* , 331, 815 (1988).
S.N. Nahar, A.K. Pradhan, W.Eissner and G.X. Chen, Phys. Rev. A, 83, 053417 (2011).
S.N. Nahar and A.K. Pradhan, *Phys. Rev. Lett.* , 116, 235003 (2016).
S.N. Nahar and A.K. Pradhan, *Phys. Rev. Lett.* 117, 249502 (2016).
Anil K. Pradhan and Sultana N. Nahar, *Atomic Astrophysics and Spectroscopy*, Cambridge University Press (2011).
A.K. Pradhan, S.N. Nahar, L. Zhao, W. Eissner, R. Trampedach and C. Orban (2017, in preparation).
F.J. Rogers and C.A. Iglesias, *Astrophys. J. Supp. Ser.* , 79, 507 (1992).
M.J. Seaton,Y. Yu, D. Mihalas and A.K. Pradhan, *Mon. Not. R. astr. Soc.* ,266,805 (1994).
The Opacity Project Team, *The Opacity Project* Vol.1 (1995); Ibid. Vol. 2 (1997), IOP Publishing, Bristol.
R. Trampedach, W. Däppen, V.A. Baturin, *Astrophys. J.* , 646, 560 (2006).
Y. Yu and M.J. Seaton, *J. Phys. B* 20, 6409 (1987).